TISSUE ENGINEERING: Part A
Volume 21, Numbers 3 and 4, 2015

DOI: 10.1089/ten.tea.2014.0269

Effects of a Ceramic Biomaterial on Immune Modulatory Properties and Differentiation Potential of Human Mesenchymal Stromal Cells of Different Origin

Giulio Bassi, PhD,[1,*] Fabien Guilloton, PhD,[2,*] Cedric Menard, PhD,[3,*] Mariano Di Trapani,[1] Frederic Deschaseaux, PhD,[2] Luc Sensebé, MD, PhD,[2] Hubert Schrezenmeier, MD, PhD,[4] Rosaria Giordano, MD, PhD,[5] Philippe Bourin, MD, PhD,[2,6] Massimo Dominici, MD,[7] Karin Tarte, PhD,[3,†] and Mauro Krampera, MD, PhD[1,†]

The aim of this study was to assess the immune modulatory properties of human mesenchymal stromal cells obtained from bone marrow (BM-MSCs), fat (ASCs), and cord blood (CB-MSCs) in the presence of a hydroxyapatite and tricalcium-phosphate (HA/TCP) biomaterial as a scaffold for MSC delivery. In resting conditions, a short-term culture with HA/TCP did not modulate the anti-apoptotic and suppressive features of the various MSC types toward T, B, and NK cells; in addition, when primed with inflammatory cytokines, MSCs similarly increased their suppressive capacities in the presence or absence of HA/TCP. The long-term culture of BM-MSCs with HA/TCP induced an osteoblast-like phenotype with upregulation of *OSTERIX* and *OSTEOCALCIN*, similar to what was obtained with dexamethasone and, to a higher extent, with bone morphogenetic protein 4 (BMP-4) treatment. MSC-derived osteoblasts did not trigger immune cell activation, but were less efficient than undifferentiated MSCs in inhibiting stimulated T and NK cells. Interestingly, their suppressive machinery included not only the activation of indoleamine-2,3 dioxygenase (IDO), which plays a central role in T-cell inhibition, but also cyclooxygenase-2 (COX-2) that was not significantly involved in the immune modulatory effect of human undifferentiated MSCs. Since COX-2 is significantly involved in bone healing, its induction by HA/TCP could also contribute to the therapeutic activity of MSCs for bone tissue engineering.

Introduction

Bone has been considered a metabolically inert tissue for a long time; actually, in adult vertebrates, it is remodeled so significantly that ~10% of the total bone content is replaced every year.[1] Bone remodeling is dependent on the dynamic balance between bone formation and resorption, which are mediated by osteoblasts and osteoclasts, respectively.[2]

The process of bone formation, namely osteogenesis, continues throughout the adult life as bone remodeling and is re-activated during fracture healing.[3] A fine regulation of this process is a prerequisite for normal bone homeostasis: Its imbalance is often linked to traumatic events or metabolic bone diseases, such as nonunion of large bone fractures or excessive bone resorption related to inflammatory bone loss.[4]

Bone regeneration may be impaired even in the absence of specific disease; for instance, 13% of tibia fractures are associated with delayed union or nonunion.[5] In addition, other conditions in orthopedic and maxillofacial surgery require a more extensive bone regeneration that the normal self-healing cannot provide; among them are the skeletal reconstruction of large bone defects related to trauma, infections, tumor resection, and skeletal abnormalities, or conditions in which the regenerative process is compromised, such as avascular necrosis and osteoporosis.[6]

[1]Stem Cell Research Laboratory, Section of Hematology, Department of Medicine, University of Verona, Verona, Italy.
[2]EFS Pyrénées Méditerranée, Université Paul Sabatier UMR5273, INSERM U1031, Toulouse, France.
[3]INSERM U917, Faculté de Médecine, Université Rennes 1, EFS Bretagne, Rennes, France.
[4]Institute of Transfusion Medicine, University of Ulm and German Red Cross Blood Donor Service Baden-Württemberg–Hessen, Ulm, Germany.
[5]Fondazione IRCCS Ca' Granda Ospedale Maggiore Policlinico, Cell Factory, Milano, Italy.
[6]CSA21, Toulouse, France.
[7]Laboratory of Cell Biology and Advanced Cancer Therapies, Department of Medical and Surgical Sciences for Children & Adults, University Hospital of Modena and Reggio Emilia, Modena, Italy.
*These authors contributed equally to this work.
†These authors contributed equally to this work and are co-corresponding authors.

Autologous bone grafting is the most common method used to treat critical-sized bone defects.[7] Bone grafts fill empty spaces and provide support to enhance the biological repair of the defect. The need for bone harvesting, which is a painful procedure associated with significant morbidity, is the main drawback of this method.[8,9] Therefore, alternative approaches of tissue engineering and new scaffolds have been developed to support bone regeneration and avoid autologous bone grafting. Indeed, bone tissue engineering (BTE) is based on the use of novel devices developed in consideration of important concepts related to bone composition and functions.[10]

Since the beginning of the 21st century, natural and synthetic polymers have been enriched with osteogenic factors to improve their mere filler properties. Bioactive factors, including bone morphogenetic proteins (BMP-2, BMP-3, BMP-4, and BMP-7), vascular endothelial growth factor (VEGF), or basic fibroblast growth factor, were used in different experimental settings in animal models.[10–12] Collagen sponges containing recombinant human BMP-2 (INFUSE®; Bone Graft, Medtronic, Minneapolis, MN) are approved for clinical use in the United States, and bovine collagen containing recombinant human BMP-7 (Osigraft; Olympus Biotech Corporation, West Lebanon, NH) has been approved by European Medicine Agency (EMA) for clinical use in Europe. The most common ceramics used in BTE include calcium sulfate and calcium phosphate, such as hydroxyapatite (HA) and β-tricalcium phosphate (β-TCP). HA and β-TCP have been approved in dental implants since the mid-1980s and are now approved for use in orthopedic implants and as bone substitutes.

BTE methods may be further improved by the employment of *ex vivo* expanded stem cells, which represent a very helpful alternative to overcome the drawbacks related to bone autograft and the use of biomaterials. In this field, mesenchymal stromal cells (MSCs) are considered a promising tool for cell therapy in regenerative medicine and for prevention or treatment of severe inflammatory and autoimmune diseases.[13] MSCs possess peculiar and multifaceted immune regulatory properties.[14–17] So far, the potential therapeutic application of MSCs for regenerative medicine and autoimmune diseases has been tested in various animal models, and it is currently under evaluation in humans. Encouraging results have been recently reported in steroid-resistant graft-versus-host disease, Crohn's disease, multiple sclerosis, kidney transplant rejection, and long bone nonunions.[18–22]

Although some reports described the role of the three-dimensional structure of biomaterials as a key regulator of MSC differentiation potential,[23,24] little data have been published on the effects of the scaffold on the MSC-mediated modulation of immune effector cells, particularly in view of allogeneic stem cell-based therapeutic strategies. Recent reports have focused on the capability of some biomaterials to interfere both *in vitro* and *in vivo* with the immune system functions, but these studies essentially relied on nonspecific assays targeting innate immunity.[25,26] Different groups worldwide have studied the immunosuppressive activity of MSCs and their anti-apoptotic effect toward various cell types, such as hematopoietic- and solid-tumor cell lines. Nevertheless, there is significant discrepancy in published data, mainly because of the lack of an international consensus on experimental conditions, procedures, and models used by different groups.[27–30] Thus, to understand whether hydroxyapatite and tricalcium-phosphate (HA/TCP) could modulate immune cell activation and survival, we used a panel of interlaboratory standardized assays to study the behavior of immune cells in contact with the scaffold.[31]

A novel biomaterial composed of HA/TCP (microporous biphasic calcium phosphate [MBCP]; Biomatlante SA, Vigneux-de-Bretagne, France) has been evaluated inside the REBORNE (Regenerating Bone defects using New biomedical Engineering approaches) European consortium (FP7-HEALTH-241879) as a suitable candidate for MSC-based BTE. Hence, we assessed the changes of immune modulatory properties, in terms of immunophenotype, suppressive, and anti-apoptotic effects of MSCs from different origin; that is, bone marrow (BM-MSCs), adipose-tissue (ASCs), and cord blood (CB-MSCs), growing in contact with HA/TCP scaffold. Moreover, we compared in different MSC types the capability of BMP-4 and dexamethasone (DXM), in the presence or absence of HA/TCP, to induce the osteoblast-like phenotype and immunomodulatory functions toward both innate and adaptive immune cells. Altogether, our data may be useful to the application of MSCs plus HA/TCP scaffold for advanced therapies of BTE in allogeneic settings.

Materials and Methods

Cell culture

Clinical-grade BM-MSCs, ASCs, and CB-MSCs were obtained in three hospital-based GMP facilities, according to standardized protocols, from healthy donors after written informed consent. Briefly, for BM-MSC isolation ($n=5$), whole BM was plated at 50,000 nucleated cells per cm^2 in closed cell culture devices (CellSTACK; Corning, Lowel, MA). Adherent cells were *ex vivo* expanded in α-minimum essential medium (α-MEM) culture medium supplemented with 5% (passage 0) and 8% (passage 1) platelet lysate (PL, Institut für Klinische Transfusionsmedizin und Immungenetik, Ulm, Germany) and 2 IU/mL heparin (Braun, Melsungen, Germany) as previously described.[32] ASCs ($n=5$) were obtained from lipo-aspirates that were enzymatically digested to obtain a single-cell suspension and plated at 50,000 nucleated cells per cm^2 in CellSTACK devices containing α-MEM culture medium supplemented with 2% apheresis-derived clinical-grade PL and 2 IU/mL heparin. CB-MSCs ($n=4$) were isolated from whole CB samples by plating cells at 50,000/cm^2 in CellSTACK devices containing SPE-IV (ABCell-Bio®; BIOSPA, Milano, Italy) culture medium supplemented with 10% fetal bovine serum (FBS; Gibco, Life Technologies, Milan, Italy). All the MSC types could be induced to differentiate into osteoblastic, chondrocytic, and adipocytic lineages and were negative for bacterial contamination; in addition, they lacked hematopoietic and endothelial marker expression (<2% cells positive for CD45, CD14, and CD31), as assessed by flow cytometry, and constantly expressed MHC-class I molecules and classical mesenchymal markers (>90% HLA-ABC-, CD73-, CD90-, and CD105-positive cells). After 10–14 days at passage 0, MSCs were trypsinized, further expanded, and frozen at the end of passage 1 to passage 3. BM-MSCs, ASCs, and CB-MSCs were thawed and plated at 1000 cells per cm^2 in the same medium used during

the *ex vivo* expansion and cultured until ~80% confluence was reached. Then, MSCs were harvested and re-seeded in parallel both in tissue culture plates and onto HA/TCP discs. HA/TCP formulation for clinical use consists of granules; to carry out the *in vitro* experiments with a standardized approach, we used some discs, obtained by mechanical pressure of the HA/TCP granules, of the diameter fitting with the wells of 24-well plates. HA/TCP ceramic discs (Micro-macroporous Biphasic Calcium Phosphate, MBCP+™, CE mark, and FDA approval) were provided by Biomatlante SA.

The HA/TCP discs are composed of HA/TCP in a 20/80 ratio according to X-ray diffraction (Rigaku Miniflex, CuK-α source). No impurities such as carbonates were detected by Fourier transformed infrared spectroscopy (Nicolet, Magnia 550). The surface morphology of the material was evaluated on samples sputter coated with gold palladium using scanning electron microscopy (LEO 1450 VP).

HA/TCP discs were inserted in ultra-low-attachment 24-well plates (Corning) to avoid attachment of MSCs to the well bottom. Briefly, after the detoxification of the biomaterial through replacement of culture media every 12 h for 2 days, MSCs were resuspended at 1×10^6/mL concentration and 200 µL of cell suspension was added to each well containing HA/TCP disc. For standard culture setting, 10^4 MSCs were seeded in 96-well flat-bottom plates. The differences in cell number between standard and HA/TCP culture conditions are related to the technical need to guarantee the same MSC/effector cell ratios regardless of the well size of culture plates. In this way, the same cell density per cm^2 was used in all culture conditions.

After a 5-day culture, half of the wells were exposed for 48 h to 10 ng/mL interferon-γ (IFN-γ) and 15 ng/mL tumor necrosis factor-α (TNF-α) (R&D Systems, Abington, United Kingdom) for inflammatory priming. Then, cells were trypsinized and harvested for subsequent phenotypic analysis. For co-culture experiments, MSCs were extensively washed with phosphate-buffered saline (PBS) to completely remove cytokines before the addition of immune cells.

Immunological phenotypic study

Unprimed and primed MSCs at passage 4 were assessed for the expression of various markers involved in cross-talk with immune cells: antigen presentation molecules HLA-ABC and CD86 from Becton Dickinson (Franklin Lakes, NJ); HLA-DR and CD80, from Beckman Coulter; and cell adhesion molecules CD54 and CD106, from Becton Dickinson. MSCs cultured on HA/TCP scaffold were harvested through repeated trypsin treatments. Trypsin activity was inhibited at the end of each cycle by adding complete culture medium. The presence of a single-cell suspension was confirmed by microscope visualization and by using forward scatter-height versus forward scatter-area to exclude doublets during fluorescence-activated cell sorting (FACS) analysis. In addition, the persistence of adherent MSCs to the biomaterial following the harvesting process was excluded by microscopy (Zeiss, Observer Z1). Two hundred thousand MSCs were pelleted, resuspended, and incubated with conjugated monoclonal antibody, following the manufacturer's instructions, for 15 min at room temperature. Then, cells were washed and analyzed by FACS Canto (Becton Dickinson) after additional TO-PRO-3 (Life Technologies) staining. A restricted phenotype (CD54, CD106, HLA-ABC, and HLA-DR expression) was used to compare the immunological phenotype of MSCs in the presence or absence of HA/TCP biomaterial. Expression was quantified as relative mean fluorescence intensity ± standard error of the mean (rMFI ± SEM).

Immunological assays

Immunological assays were performed as previously standardized.[31] Buffy coats were obtained from Transfusion Center (AOUI, Verona, Italy) and processed to obtain peripheral blood mononuclear cells (PBMC, $n = 15$). Then, T, B, or NK cells were purified by negative selection with magnetic beads (magnetic activating cell sorting; Miltenyi Biotec, Cologne, Germany), following the manufacturer's instructions. Only products with purity >95% and viability >98% were cryopreserved and used for subsequent experiments. Both MSC cell batch and immune effector cell variability were considered, and the immunomodulatory properties of MSCs were tested on a number of PBMC donors ($n = 15$) to obtain consistent data. Thawed T ($n = 5$), B ($n = 5$), and NK ($n = 5$) cells were resuspended in appropriated culture medium. For T cells, RPMI 1640 (Gibco, Life Technologies) was supplemented with 10% Human AB Serum (Institut Jacques Boy, Reims, France); for B cells, RPMI 1640 was supplemented with 10% Australian-selected FBS (Gibco, Life Technologies); and for NK cells, IMDM (Gibco, Life Technologies) was supplemented with 10% Human AB Serum.

T,- B-, and NK-cell proliferation was assessed with carboxyfluorescein-diacetate-succimidyl-ester method (CFSE; Gibco, Life Technologies). CFSE-labeled cells were seeded on MSCs at passage 4 and were previously plated in 96-well flat-bottom plates or in 24-well ultra-low attachment plates + HA/TCP, at different ratios (10:1 for T:MSCs, 1:1 for NK:MSCs and B:MSCs). Then, nonantigen-specific stimuli were added to culture to address the effect of MSCs on the different immune effector cell proliferation. T cells were activated with 0.5 µg/mL cross-linking anti-CD3 and anti-CD28 antibodies (Sanquin, Amsterdam, The Netherlands) for 6 days. B cells were activated with 2 µg/mL $F(ab')_2$ anti-human IgM/IgA/IgG antibody (Jackson Immunoresearch, Suffolk, United Kingdom), 50 IU/mL interleukin-2 (IL-2, Proleukin®; Novartis, Basel, Switzerland), 0.5 µg/mL polyhistidine-tagged CD40 ligand, 5 µg/mL anti-polyhistidine cross-linking antibody (R&D Systems), and 0.5 µg/mL CpG B (ODN 2006; Invivogen, Toulouse, France) for 4 days. NK cells were activated with 100 IU/mL IL-2 for 6 days. At the end of co-culture, cells were trypsinized, stained with TO-PRO-3 (Life Technologies), CD45-PerCP (Beckton Dickinson), and acquired by a flow cytometer. Proliferation was assessed by CFSE dilution of $CD45^+$ cells using FlowJo software (TreeStars, La Jolla, CA), and percentage of viable cells undergoing more than one cell division was considered for quantification of immunosuppressive properties of MSCs by means of the following formula: percentage of inhibition of proliferation = (percentage proliferation of lymphocytes without MSCs − percentage proliferation of lymphocytes with MSCs)/(percentage proliferation of lymphocytes without MSCs)*100.

In some experiments, specific inhibitors of immunosuppressive molecular pathways were added to MSC/T cell

coculture, that is, 1 mM L-1-methyltryptophan (L-1MT; Sigma-Aldrich, Milan, Italy), 5 μM NS-398 (Cayman Chemicals, Ann Arbor, MI), and 10 μg/mL of IFN-γ blocking antibody (Becton Dickinson).

To determine the anti-apoptotic features of MSCs, unstimulated lymphocytes were seeded either alone or at different ratios with BM-MSCs, ASCs, and CB-MSCs. T cells were co-cultured at a T:MSC ratio of 10:1, while B and NK cells were cocultured at 1:1 (B or NK:MSC). After 4 days (B and NK cells) or 6 days (T cells) of co-culture, cells were harvested by trypsinization and stained with CD45-APC antibody (Becton Dickinson). After centrifugation, the supernatant was discarded and the cell pellet was fixed with CytoFix/CytoPerm (Becton Dickinson) for 20 min at 4°C. Then, cells were washed with Perm&Wash Buffer (Becton Dickinson), stained with anti-active-caspase-3-PE (Becton Dickinson), and analyzed by flow cytometry.

Osteogenic differentiation

Sub-confluent BM-MSCs, ASCs, and CB-MSCs cultured in 24-well plates with or without HA/TCP discs were treated for 21 days with osteogenic medium. Two differentiation media were tested, both of which contained not only a common osteogenic cocktail including α-MEM, 2% FBS, 1 mM β-glycerophosphate (Sigma-Aldrich), and 50 μM ascorbic acid, but also either 0.1 μM DXM (Sigma-Aldrich) or 50 ng/mL BMP-4 (R&D System). Differentiation media were replaced twice a week. At the end of culture, some wells were selected for the immunological studies previously described, by using the same immune cell batches. Supernatants were stored at −20°C to assess cytokine production and tryptophan/kynurenin ratio, as previously described.[31] Other wells were treated with Trizol Reagent (Invitrogen, Life Technologies, Torino, Italy) for RNA extraction and quantitative real-time polymerase chain reaction (RT-qPCR). Some other wells were selected for colorimetric assays to confirm the differentiation of cultured cells, including alkaline phosphatase (ALP), Alizarin Red (AR) staining, and Von Kossa (VK) staining. Briefly, cells were fixed with 4% paraformaldehyde (Sigma-Aldrich) for 30 s at room temperature. Then, for ALP staining, a solution containing New Fucsin (Sigma-Aldrich) in Propanediol buffer supplemented with naphtol-ASBI-phosphate (Sigma-Aldrich) was added to wells, incubated for 30 min under stirring, and washed thrice with PBS. For AR staining, cells were incubated for 10 min with AR solution under stirring (AR 2%, pH 4.1) and washed thrice with deionized water to remove unspecific staining. For VK staining, cells were exposed to light for 1 h in the presence of 10% solution of silver nitrate (Sigma-Aldrich). After washing with deionized water, the wells were incubated with sodium thiosulfate solution 10% (Sigma-Aldrich) for 5 min. Stained cells were acquired by an inverted microscope (Zeiss, Observer Z.1) at 10× magnification.

Quantitative PCR

Cells were lysed using Trizol reagent (Life Technologies), and RNA was extracted following the manufacturer's protocol. Total RNA (2 μg) was then cleaned up using RNeasy Mini kit (Qiagen, Limburg, The Netherlands) to discard DNA and solvent contamination according to RNA clean-up protocol. RNA purity and integrity was checked using the Experion™ RNA Std Sens Reagents on the Experion automatized system (Bio-Rad, Hercules, CA). All samples used for cDNA synthesis displayed an RNA integrity number above 9. Whole purified RNA was then reverse transcribed by the PrimeScript RT-PCR kit (Takara Bio, Inc., Otsu, Japan). Quantitative PCR was performed on diluted cDNA (equivalent to 25 ng of starting purified RNA) using SSoFast EvaGreen Supermix (Bio-Rad) with 500 nM of forward and reverse primers in a total volume of 20 μL on a CFX™ Real Time System (Bio-Rad) as follows: 95°C, 3 min, and 40 cycles of denaturation (95°C, 10 s) and primers hybridation and amplification (60°C, 30 s). Primer sequences are listed in Supplementary Table S1 (Supplementary Data are available online at www.liebertpub.com/tea).

Each primer couple displayed interpretable PCR efficiency (95–105%). Melt curves and appropriate controls were used to validate amplification specificity. Data were analyzed on Bio-Rad CFX manager (threshold = 0.2) and exported to DataAssist Software v3.0 (Applied Biosystems, Foster City, CA). Gene expression was calculated using the fold change of $2^{-\Delta\Delta Ct}$ method using GAPDH as an appropriate reference gene with the smallest M score.

Western blotting

For total protein lysate, cells were lysed with sodium deoxycholate (DOC) 5% w/v (Calbiochem, Billerica, MA) in ddH_2O supplemented with Complete Protease Inhibitor (Sigma-Aldrich). In order to quantify protein lysate, the BCA protein assay kit (Bicinchoninic Acid Assay, Thermo Scientific, Waltham, MA) was used according to the manufacturer's instructions. Then, 20 μg of protein lysate were resolved by sodium dodecyl sulfate–polyacrylamide gel electrophoresis (SDS-PAGE), and blotted on a 0.45 μm nitrocellulose filter for further analysis.

Anti-RunX2, anti-NF-κB, anti-phospho-NF-κB, and anti-phospho-Smad-1, -5, and -8 (all from Cell Signaling, Danvers, MA) were used at 1:5000 dilution; instead, β-actin (Sigma-Aldrich) was used at 1:30,000 dilution. Secondary antibodies were anti-mouse, anti-goat (both from Sigma-Aldrich), and anti-rabbit (GE Healthcare, Pittsburgh, PA) labeled with ALP or horseradish peroxidase, all of which were used at 1:10,000 working dilution.

For quantification of RunX2 expression, relative protein level was referred to β-actin using Imagej densitometric software plugins.

Results

Lymphocyte behavior and MSC phenotype in presence of HA/TCP

We analyzed the survival of unstimulated purified T, B, and NK cells after 4–6 days of co-culture with HA/TCP discs. As shown in Figure 1A, lymphocyte spontaneous apoptosis rate was not modified by the presence of biomaterial. Moreover, neither cell activation nor proliferation of unstimulated CFSE-labeled immune cells was observed (data not shown). Similarly, HA/TCP discs did not modify immune cell proliferation, as assessed by comparing the percentage of cells undergoing at least one division with or without HA/TCP (Fig. 1B). These data confirm previous reports on the

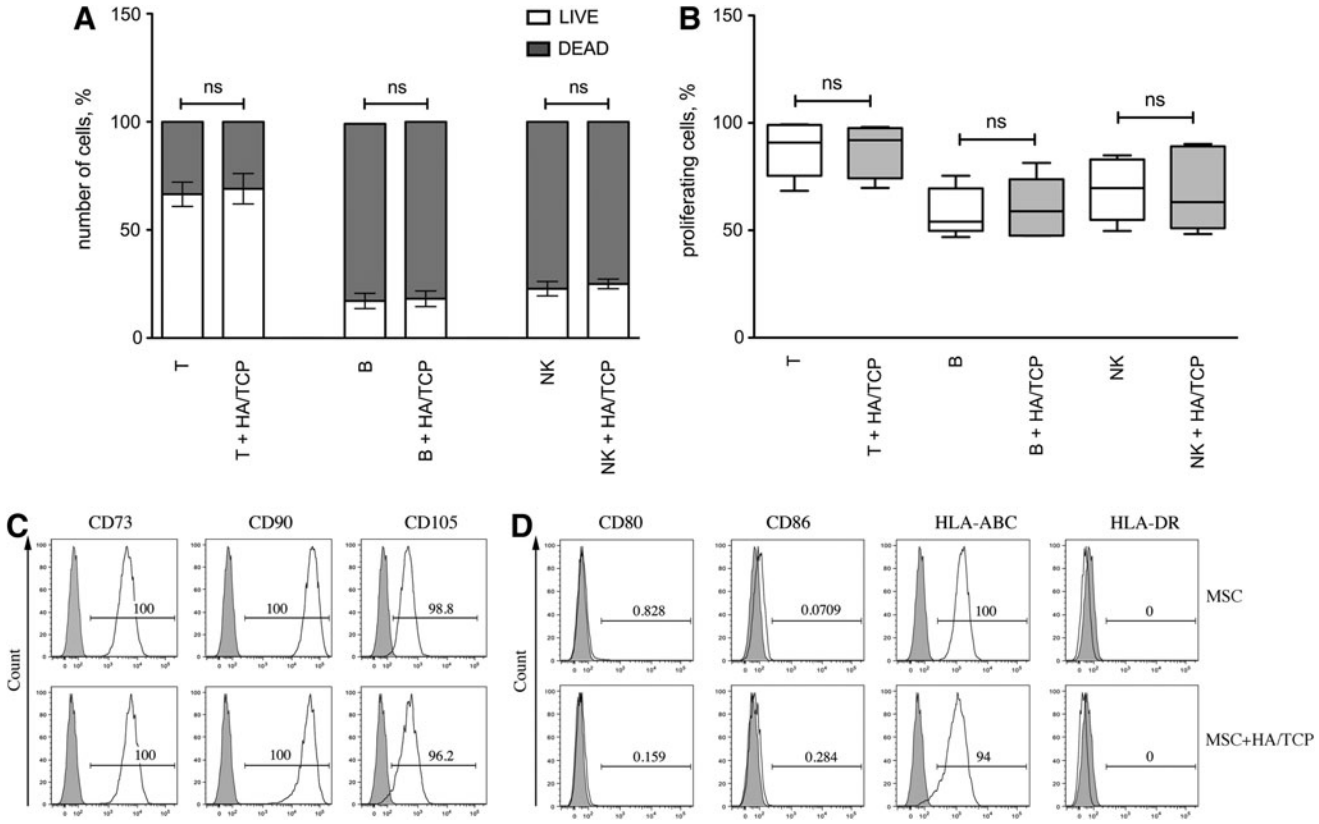

FIG. 1. Effect of hydroxyapatite (HA)/tricalcium-phosphate (TCP) discs on survival and proliferation of T, B, and NK cells. **(A)** Relative percentage of live ($CD45^+$/active-caspase 3^-) and dead cells ($CD45^+$/active-caspase 3^+) after culture in absence or presence of HA/TCP discs ($n=8$); **(B)** Percentage of live CFSE-labeled dividing cells after 4–6 days of culture in absence or presence of HA/TCP ($n=8$); **(C)** mesenchymal stromal cells (MSCs) were collected after 5 days of culture in absence or presence of HA/TCP and stained with appropriate antibodies (empty histogram) or isotype-matched controls (*gray histogram*). One bone marrow (BM)-MSC sample, representative of 14 MSC batches (5 BM-MSCs, 5 ASCs, and 4 cord blood [CB]-MSCs), is shown for MSC-related markers and, in **(D)**, for immunological markers. Wilcoxon paired test was used to compare different groups, ns $p>0.05$.

biocompatibility of HA/TCP materials and foster their usefulness as a bone defect filler in clinical practice.

Then, we asked whether the presence of HA/TCP could affect the immunophenotypic pattern of MSCs of different origins. First, we found that MSCs could be cultured without alteration of cell growth in association with HA/TCP discs and harvested at 7 days after culture. The selection of markers was based according to the minimal criteria to define MSCs.[33] As shown in Figure 1C, BM-MSCs expressed CD73, CD90, and CD105, without any difference related to presence of the scaffold. Similar marker expression was found in ASCs and CB-MSCs (data not shown). We then analyzed the expression of molecules related to the immunological behavior of MSCs by studying in parallel the immune phenotype of both resting (Fig. 1D) and IFN-γ/TNF-α-primed MSCs (data not shown). Even in the presence of biomaterial, all MSC types were negative for the expression of CD80, CD86, and HLA-DR. As expected, HLA-ABC molecules were always detected on MSC surface at a different intensity depending on cell origin and expansion medium employed (Table 1). CB-MSCs expressed a lower level of HLA-ABC in resting and primed conditions, as compared with BM-MSCs or ASCs. ASCs and CB-MSCs never expressed CD106 in resting conditions, but it was *de novo* expressed after inflammatory priming and could also be upregulated in BM-MSCs, thus confirming previous data from our group.[31] CD54 was already expressed, regardless of the presence of HA/TCP and was induced after inflammatory priming. Moreover, the upregulation of HLA-ABC molecules and the *de novo* expression of HLA-DR were also observed in BM-MSCs and ASCs even in contact with biomaterial. CB-MSCs showed lower HLA-DR expression after inflammatory priming, as compared with the other MSC types. In summary, the association of MSCs with HA/TCP, mimicking the natural composition of bone tissues, did not significantly modify the expression of immunological markers on MSCs.

Anti-apoptotic and immune modulatory properties of BM-MSCs, ASCs, and CB-MSCs in presence of HA/TCP scaffold

We compared the survival of immune effector cells in co-culture with different MSC types in the absence or presence of HA/TCP scaffold. As shown in Figure 2A, the combination of BM-MSCs, ASCs, and CB-MSCs with HA/TCP did not affect their anti-apoptotic properties toward lymphocytes. Co-culture with all MSC types significantly increased B- and NK-cell survival, regardless of the presence of the

Table 1. Comparative Analysis of BM-MSCs, ASCs, and CB-MSCs Phenotype After Culture in Absence or Presence of HA/TCP Discs

	BM-MSCs only	*BM-MSCs+HA/TCP*	*ASCs only*	*ASCs+HA/TCP*	*CB-MSCs only*	*CB-MSCs+HA/TCP*
CD54	4.51 ± 0.50	2.69 ± 0.50	6.3 ± 0.59	4.43 ± 0.54	9.5 ± 0.42	9.54 ± 0.23
	1023.24* ± 228.40	**884.53* ± 348.20**	**429.06* ± 113.03**	**623.95* ± 108.05**	**474.73* ± 24.13**	**490.51* ± 21.16**
CD106	4.22 ± 1.15	3.54 ± 1.14	1	1	1 ± 0.11	1
	24.54* ± 3.05	**20.20* ± 6.01**	**7.72* ± 1.57**	**9.24* ± 0.76**	**3.53* ± 0.26**	**3.85* ± 0.31**
HLA-ABC	24.86 ± 2.36	20.49 ± 2.60	19.96 ± 2.44	20.62 ± 1.82	3.92 ± 0.25	3.92 ± 0.20
	92.61* ± 31.20	**91.26* ± 16.40**	**42.50* ± 7.30**	**45.25* ± 5.57**	**11.08* ± 0.51**	**12.09* ± 0.95**
HLA-DR	1	1	1	1	1	1
	58.45* ± 4.60	**46.68* ± 25.00**	**4.09* ± 0.37**	**3.84* ± 0.41**	**2.02* ± 0.10**	**2.02* ± 0.21**

MSCs ($n = 14$) were stimulated or not by IFN-γ + TNF-α for 48 h in absence or presence of HA/TCP discs. Cells were collected, stained with appropriate antibody, and analyzed by flow cytometry. Data were represented as rMFI ± SEM of resting MSCs and primed MSCs (bold). Nonparametric paired Wilcoxon test was used to compare different groups.

*$p < 0.05$.

BM, bone marrow; CB, cord blood; HA, hydroxyapatite; IFN-γ, interferon-γ; MSC, mesenchymal stromal cell; rMFI, relative mean fluorescence intensity; SEM, standard error of the mean; TCP, tricalcium-phosphate; TNF-α, tumor necrosis factor-α.

HA/TCP scaffold. As expected, T-cell survival was only slightly increased by the co-culture with MSCs, considering their lower spontaneous apoptosis rate as compared with B or NK cells.

In view of producing data for the clinical application of MSCs in association with HA/TCP, we asked whether the presence of the biomaterial could affect the immune modulatory properties of MSCs of different origin. BM-MSCs, ASCs, and CB-MSCs were co-cultured with stimulated T, B, and NK cells in the presence (gray box) or absence (white box) of HA/TCP scaffold. As shown in Figure 2B, ASCs displayed the strongest suppressive capabilities on T-cell proliferation, as compared with BM-MSCs and CB-MSCs. Notably, primed BM-MSCs (pBM) showed similar inhibitory properties as resting and primed ASCs (pASC), while inflammatory priming only slightly increased CB-MSC (pCB) immune modulation.

Resting ASCs, even when associated with the scaffold, supported B-cell proliferation. In contrast, resting BM-MSCs and CB-MSCs neither supported nor significantly inhibited B-cell proliferation. With the exception of CB-MSCs, all inflammatory-primed MSCs suppressed B-cell proliferation by more than 50%.

IL-2-mediated NK-cell proliferation was similarly inhibited by BM-MSCs, ASCs, and CB-MSCs and this effect was increased after priming with inflammatory cytokines, especially for BM-MSCs.

We also investigated the molecular mechanisms underlying MSC-mediated immunosuppression. The inhibition of T-cell proliferation was driven, both in standard culture setting and in the presence of HA/TCP, by the activation of indoleamine-2,3 dioxygenase (IDO), as shown by the addition of its specific inhibitor L-1MT (Fig. 2C). We previously demonstrated that IDO induction was mostly dependent on IFN-γ release by T cells,[27] and in agreement, T-cell inhibition by MSC was partially reversed by IFN-γ blocking antibody; whereas the prostaglandin E2 (PGE2) specific inhibitor NS-398 had no effect (Fig. 2C). To further confirm this observation, we quantified the concentration of tryptophan and kynurenine in culture supernatants, demonstrating that inflammatory priming led to a similarly strong activation of IDO regardless of the presence or not of HA/TCP discs (Fig. 2D).

Overall, HA/TCP biomaterial did not modify the typical MSC immunological functions and the molecular mechanisms involved.

Osteoblastic differentiation potential of BM-MSCs, ASCs, and CB-MSCs in presence of HA/TCP discs

We compared the efficacy of two different media, that is, dexamethasone-based medium (DXM) and BMP-4-based medium (BMP-4), to induce the osteoblast-like phenotype in BM-MSCs, ASCs, and CB-MSCs. After 21 days of culture in osteogenic medium, we found that DXM could induce distal-less homeobox-5 (*DLX5*) expression in all MSC types employed, but triggered only slight mineralization in ASCs (Figs. 3 and 4A). Conversely, BMP-4 efficiently promoted calcium nodule deposition in BM-MSCs, CB-MSCs, and, to a lesser extent, in ASCs.

The analysis of mRNA transcription by RT-qPCR revealed that BM-MSCs were the most prone in activating osteoblastic-related genes, such as *DLX5*, parathyroid hormone receptor 1 (*PTHR1*), osterix (*OSX*), and osteocalcin (*OSC*) (Fig. 4A). As previously demonstrated,[12] we confirmed that BMP-4 could improve the differentiation of BM-MSCs. Moreover, BMP-4-based medium could also induce the transcription of *DLX5*, *PTHR1*, and *OSX* in CB-MSCs and ASCs. The association of BM-MSCs with HA/TCP showed a synergistic effect with BMP-4, as demonstrated by the increase in *OSC* expression, which encodes a protein related to the mature osteoblastic phenotype (Fig. 4B). Interestingly, culturing BM-MSCs with HA/TCP triggered by itself the transcription of *OSC* and *OSX* genes, without the need of any differentiation inducers, thus demonstrating osteo-inductive properties of HA/TCP material (Fig. 4C).

We then performed western blotting analysis of runt-related transcription factor 2 (RUNX2) expression, one of the central tissue factors involved in osteogenic differentiation process. As shown in Figure 4D and E, RUNX2 was detected in BM-MSCs even without any differentiation stimulus. ASCs expressed low RUNX2 as compared with BM-MSCs, and in CB-MSCs the expression of RUNX2 was variable among different batches. RUNX2 expression could be induced at protein level by the treatment with

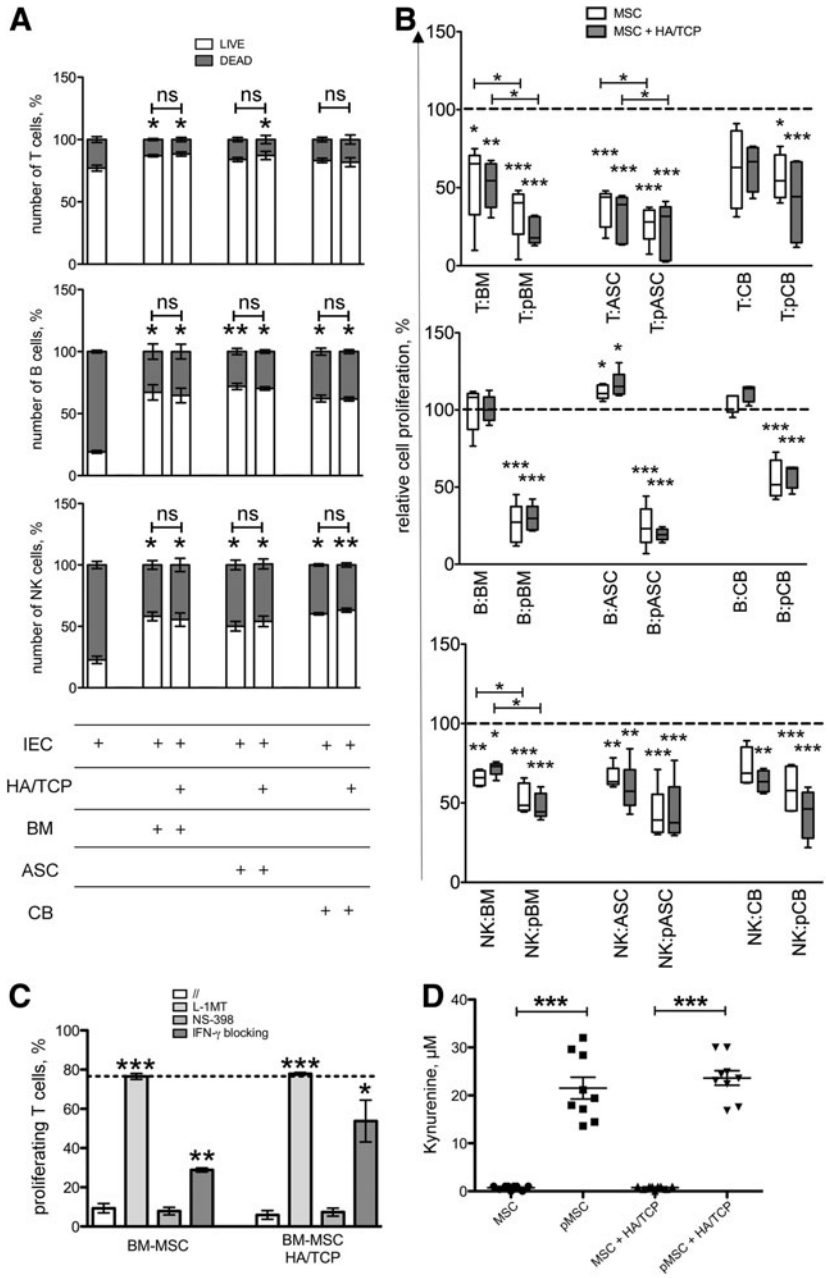

FIG. 2. Immune modulatory features of BM-MSCs, ASCs, and CB-MSCs toward different immune effector cells in presence of HA/TCP scaffold. **(A)** Immune effector cells (IEC) were co-cultured in absence or presence of BM-MSCs ($n=5$), ASCs ($n=5$), and CB-MSCs ($n=4$), and seeded in standard culture setting or in presence of HA/TCP. After 4–6 days of co-culture, T, B, and NK cells were collected and stained with anti-CD45-APC and active-caspase-3 antibody-PE. Percentages of live (*clear histograms*) and dead (*gray histograms*) cells were calculated on total $CD45^+$ events. **(B)** CFSE-labeled T, B, and NK cells were stimulated and co-cultured with different MSC types (BM, ASC, CB, and interferon-γ (IFN-γ) + tumor necrosis factor-α (TNF-α) treated MSC: pBM, pASC, and pCB) in a standard culture setting and in combination with HA/TCP discs. After 4–6 days of co-culture, cells were collected and stained with CD45-PerCP and TO-PRO-3. Percentage of divided cells in absence of MSCs was set as 100% (*dotted lines*), and each condition was normalized on this value. Relative proliferation of immune effector cells in co-culture with MSCs of different origins in a standard culture setting (*white box*) was analyzed in parallel with the relative proliferation in co-culture with different MSC types in association with HA/TCP discs (*gray box*). **(C)** CFSE-labeled T cells were stimulated and co-cultured with BM-MSCs ($n=5$) in presence of L-1MT, NS-398, and anti-IFN-γ blocking antibody in standard culture condition and in presence of HA/TCP scaffold. After 6 days of co-culture, cells were collected and stained with CD45-PerCP and TO-PRO-3. The percentage of live T cells that underwent at least one cell division was represented in each condition. *Dotted line* represented the mean of divided T cells in absence of MSCs. **(D)** MSCs ($n=9$) were stimulated or not by IFN-γ + TNF-α for 48 h in absence or presence of HA/TCP discs. Culture supernatants were collected for indoleamine-2,3 dioxygenase (IDO) activity quantification by HPLC. One-way ANOVA test was used to compare different groups. ns $p>0.05$; *$p<0.05$; **$p<0.01$; and ***$p<0.001$.

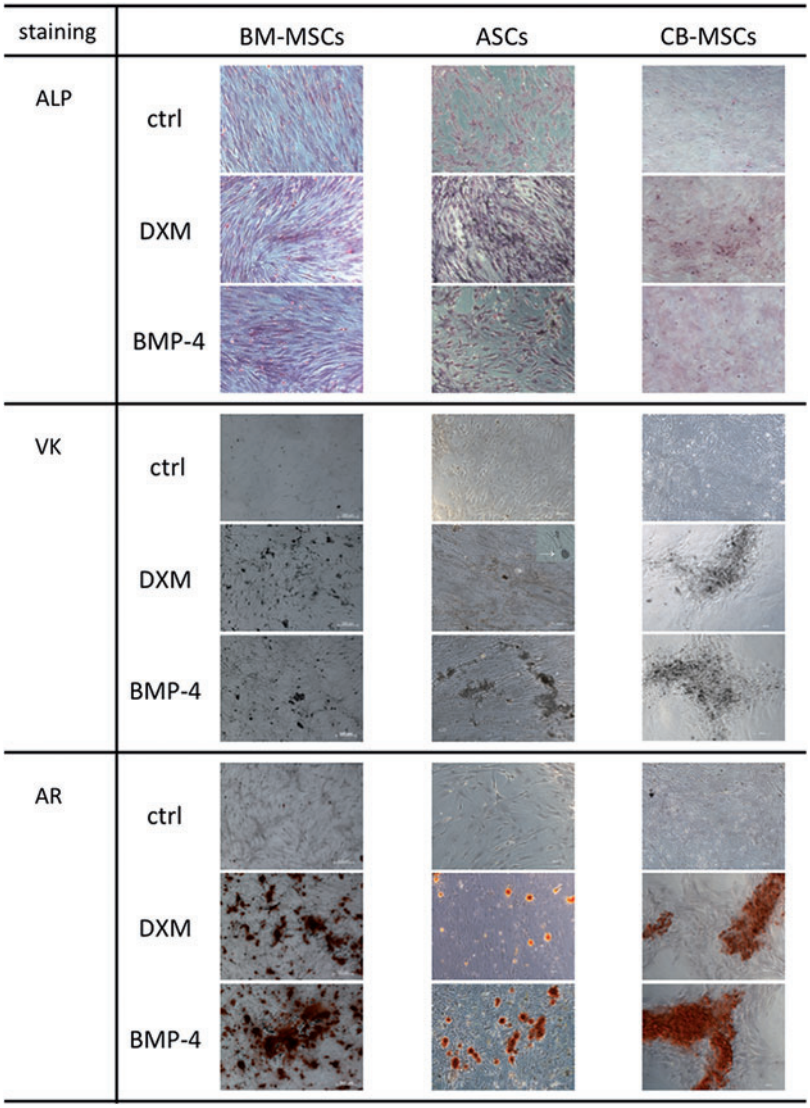

FIG. 3. Differentiation potential of BM-MSCs, ASCs, and CB-MSCs in presence of dexamethasone (DXM) or bone morphogenetic protein 4 (BMP-4) in standard culture conditions. After a 21 day culture in osteogenic medium, cells were fixed and stained for determination of alkaline phosphatase activity (*upper*), mineral deposition through Von Kossa (VK) staining (*middle*; representative image of lipid droplet detection in ASCs as indicated by the *arrow*), and calcium nodule formation by means of Alizarin Red (AR) staining (*lower*). Images were acquired by Axiovert Z1 microscope (Zeiss) at 10× magnification. The representative images are derived from five different donors for BM-MSCs, five different donors for ASCs, and four different donors for CB-MSCs. Color images available online at www.liebertpub.com/tea

DXM or BMP-4 in BM-MSCs and CB-MSCs; while in ASCs, RUNX2 expression was only slightly upregulated. Altogether, these data suggest that HA/TCP biomaterial favored osteogenic commitment of MSCs whatever the differentiation medium, at both transcriptional and protein levels.

Immune modulatory properties of BM-MSCs, ASCs, and CB-MSCs after osteoblastic differentiation

Considering the superiority of BMP-4 compared with DXM in promoting osteoblast-like phenotype, we asked whether the MSC osteogenic commitment, induced by either HA/TCP or HA/TCP supplemented with BMP-4, could modulate their immunological properties, thus inducing immune effector cell activation that could theoretically lead to implant rejection. For that purpose, we applied our validated immunological assays to MSCs maintained in the presence of biomaterial and osteogenic medium for 26 days, supplemented or not with BMP-4. At the end of differentiation, half of the wells were treated with IFN-γ and TNF-α, as previously described. We found that BM-MSCs, ASCs, and CB-MSCs associated with HA/TCP or with HA/TCP+BMP-4 did not induce spontaneous immune cell proliferation (data not shown) and retained their supportive effects by preventing spontaneous B- and NK-cell apoptosis (Fig. 5A). Only BMP-4-differentiated CB-MSCs maintained their inhibitory effect on T- and NK-cell proliferation and, after inflammatory priming, on B-cell proliferation (Fig. 5B). Conversely, differentiated ASCs lost their capacity to inhibit NK-cell proliferation in unprimed conditions, but this potential was restored after inflammatory priming.

The most important differences were found with both BM-MSCs and BMP-4-differentiated BM-MSCs in association with HA/TCP for long-term culture (26 days); in fact, BM-MSCs lost their capability to inhibit NK-cell proliferation, even after inflammatory priming, while T-cell proliferation was still inhibited without any further increase after inflammatory priming. On the other hand, the capability of IFN-γ/TNF-α-primed, BMP-4 differentiated BM-MSCs to suppress B-cell proliferation was not affected.

IDO activation also maintained its central role in inhibiting T-cell proliferation in BMP4-differentiated MSCs. However, NS-398, the specific inhibitor of cyclooxygenase 2 (COX-2) pathway, partially restored the proliferation of

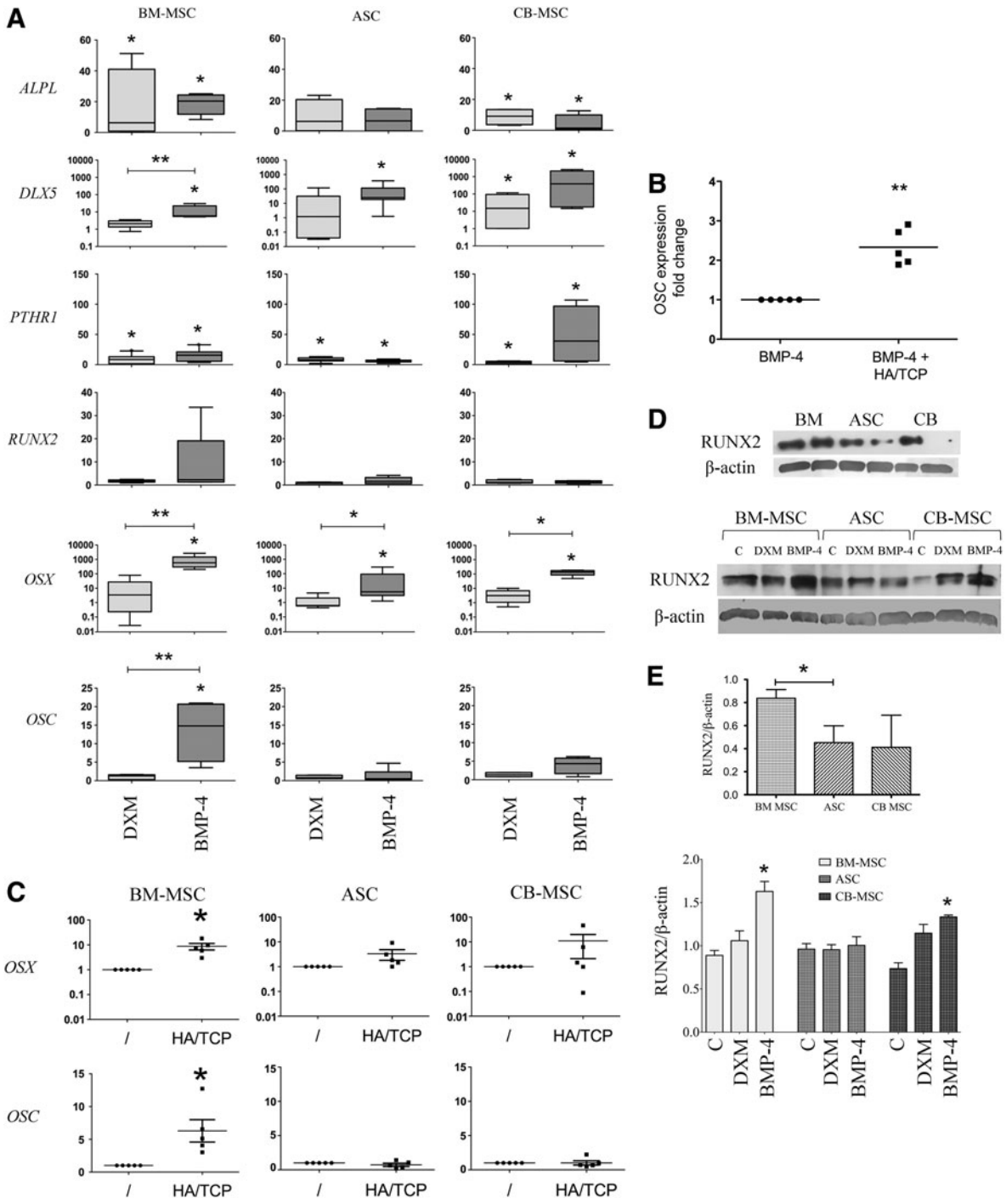

FIG. 4. Osteoblastic differentiation of BM-MSCs, ASCs, and CB-MSCs with DXM or BMP-4-inducing media in a standard culture setting and in presence of HA/TCP scaffold. **(A)** BM-MSCs, ASCs, and CB-MSCs were cultured for 21 days in presence of osteogenic medium supplemented with dexamethasone or BMP-4. Relative gene expression was represented as fold change (Y axis) as compared with control condition without inducers. **(B)** Synergistic effect of HA/TCP discs on osteocalcin (OSC) expression in BM-MSCs. Y axis represents fold change of *OSC* gene expression in BM-MSCs + BMP-4 in association with HA/TCP as compared with BM-MSCs cultured in presence of BMP-4 in a standard culture setting. **(C)** Osterix and osteocalcin relative expression in BM-MSCs, ASCs, and CB-MSCs cultured in presence of HA/TCP, as compared with cells cultured in standard culture conditions, in absence of dexamethasone and BMP-4 addition. **(D)** Western blotting analysis of runt-related transcription factor 2 (RUNX2) expression of MSCs cultured in expansion medium, according to each cell factory protocol (*upper panel*). Western blotting analysis of RUNX2 protein expression after 21 days of culture in differentiation medium containing DXM or BMP-4 in BM-MSCs, ASCs, and CB-MSCs. β-actin was used as loading control. **(E)** Quantification of RUNX2 expression in expanded MSCs (BM-MSC, $n=3$; ASC $n=3$; CB-MSC $n=3$) and in differentiated MSCs (BM-MSC, $n=3$; ASC $n=3$; CB-MSC $n=3$). For quantification of RUNX2 expression, relative protein level was normalized to β-actin. Nonparametric paired Wilcoxon test was used to compare different groups. $^{*}p<0.05$ and $^{**}p<0.01$.

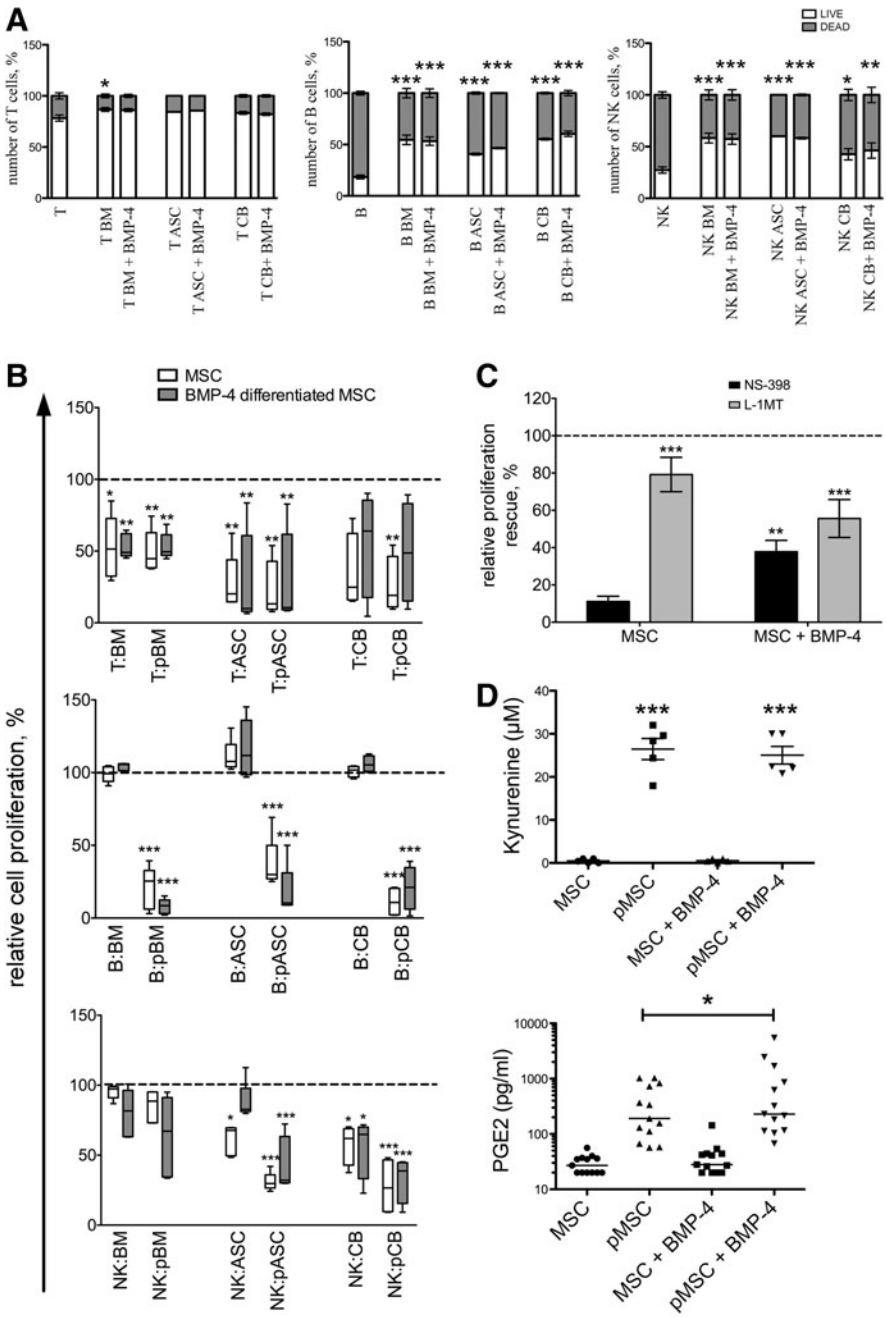

FIG. 5. Immune modulatory features of predifferentiated BM-MSCs, ASCs, and CB-MSCs toward different immune effector cells in presence of HA/TCP scaffold. **(A)** After differentiation process of MSCs, purified T, B, and NK cells were thawed and seeded in 24-well plates in presence of undifferentiated or BMP-4-differentiated MSCs. After 4–6 days of co-culture T, B, and NK cells were collected and stained with anti-CD45-APC and active-caspase-3 antibody-PE. Percentage of live (*clear histograms*) and dead (*gray histograms*) cells was calculated in total $CD45^+$ events. **(B)** CFSE-labeled T, B, and NK cells were stimulated and co-cultured with undifferentiated and predifferentiated BM-MSCs, ASCs, and CB-MSCs. After 4–6 days of co-culture, cells were collected and stained with CD45-PerCP and TO-PRO-3. Percentage of dividing cells in absence of MSCs was set as 100% (*dotted lines*), and each condition was normalized on this value. Relative proliferation of immune effector cells in co-culture with undifferentiated MSCs (*white box*) was analyzed in parallel with the relative proliferation in co-culture with BMP-4-differentiated MSCs (*gray box*). The data obtained are represented as relative proliferation of stimulated-T, -B, or -NK cells in comparison with the control condition (immune effector cells without MSCs). **(C)** CFSE-labeled T cells were stimulated and co-cultured with undifferentiated and predifferentiated BM-MSCs in presence of L-1MT and NS-398. After 6 days of co-culture, cells were collected and analyzed by means of flow cytometry. Percentage of dividing cells in absence of MSCs was set as 100% (*dotted lines*), and each condition was normalized to this value. The percentage of proliferation of T cells co-cultured with MSCs in absence of inhibitor was considered as zero. Relative rescue of proliferation was calculated by comparing the percentage of divided cells with the control. **(D)** Culture supernatants of differentiated and/or primed BM-MSCs ($n=5$) were collected for IDO activity quantification by HPLC and for prostaglandin E2 (PGE2) quantification by ELISA assay. One-way ANOVA test was used to compare different groups; $*p<0.05$; $**p<0.01$; and $***p<0.001$.

T cells when co-cultured with BMP-4-differentiated BM-MSCs (Fig. 5C). We then evaluated IDO and COX-2 activation by measuring kynurenine and PGE2 production in cell supernatants (Fig. 5D). The differentiation of BM-MSCs did not alter the capability of IFN-γ and TNF-α to induce IDO activation; however, osteoblastic differentiation induced by BMP-4 increased PGE2 production and prostaglandin-endoperoxide synthase 2 (*PTGS2*) transcription in primed BM-MSCs, thus confirming the synergistic role of COX-2 pathway with IDO in BMP-4-differentiated MSCs (Fig. 6A).

We then assessed whether inflammatory priming could affect differentiation and activation state of MSCs. The treatment with inflammatory cytokines reduced RUNX2 expression at both mRNA (Fig. 6B) and protein levels, in both DXM- and BMP-4-treated MSCs. Moreover, inflammatory priming suppressed the BMP-4-mediated activation of Smad-1, -5, and -8 and the shift to the TNF-α-related NF-κB phosphorylation (Fig. 6C). Thereafter, osteogenic differentiation of BM-MSCs is linked to changes of immunoregulatory functions, which are partially restored by the exposure to the inflammatory milieu.

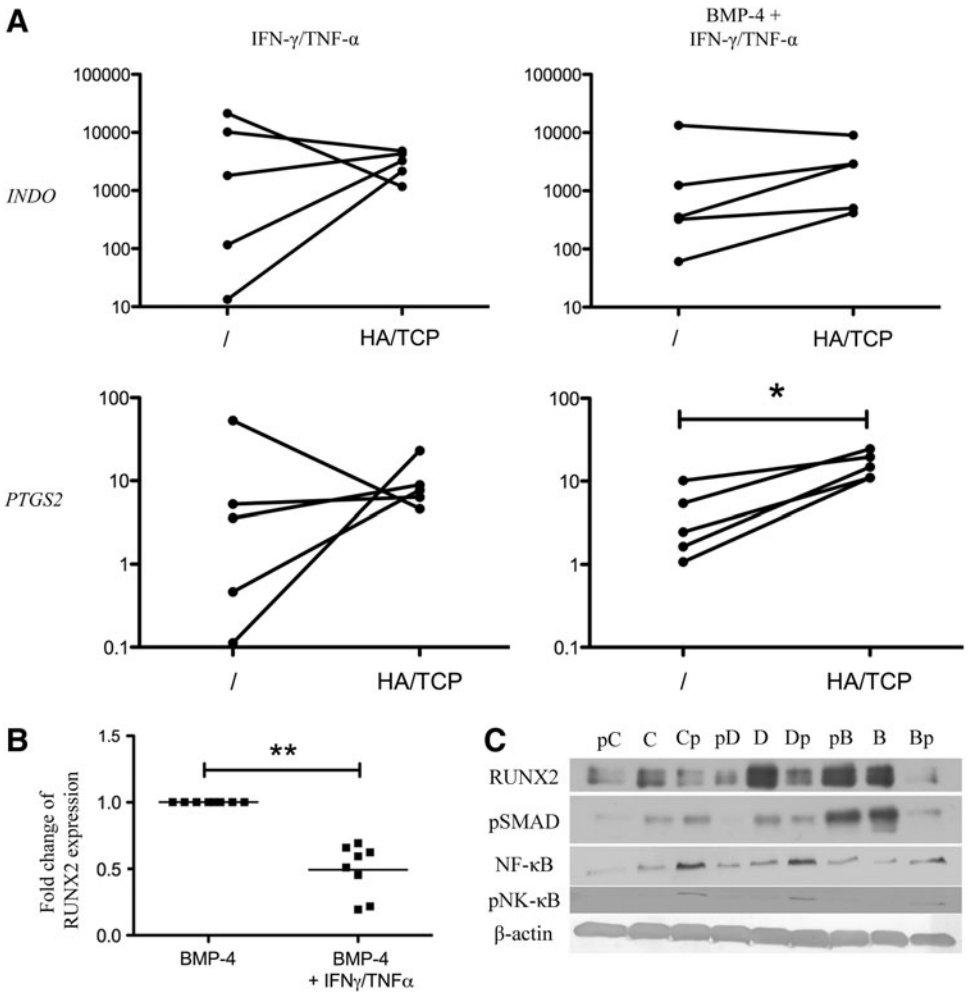

FIG. 6. *IDO1* and prostaglandin-endoperoxide synthase 2 (*PTGS2*) expression in primed BM-MSCs in control medium or in presence of BMP-4. **(A)** BM-MSCs were cultured for 21 days in presence of either osteogenic medium alone or supplemented with BMP-4. After differentiation process, cells were cultured for 48 h with inflammatory cytokines before RNA extraction. Relative gene expression is represented (Y axis) using *GADPH* as a reference gene. **(B)** Effect of inflammatory priming on *RUNX2* expression in BM-MSCs cultured for 21 days in presence of BMP-4. After differentiation process, cells were exposed to inflammatory cytokines for 48 h before RNA extraction. Relative gene expression is represented as fold change (Y axis) as compared with *GADPH* expression. **(C)** Western blotting analysis of RUNX2, NF-κB, phospho-NF-κB, and phospho-Smad-1, -5, and -8 expression in BM-MSCs. After 21 days of induction with either control medium, DXM-based medium or BMP-4-based medium, cells were lysed and proteins were collected and detected through sodium dodecyl sulfate–polyacrylamide gel electrophoresis (SDS-PAGE). β-Actin was used as loading control. One representative experiment was shown for BM-MSCs. pC = 48 h IFN-γ and TNF-α + 21 days control medium; C = 21 days control medium; Cp = 21 days control medium + 48 h IFN-γ and TNF-α; pD = 48 h IFN-γ and TNF-α + 21 days DXM-based medium; D = 21 days DXM-based medium; Dp = 21 days DXM-based medium + 48 h IFN-γ and TNF-α; pB = 48 h IFN-γ and TNF-α + 21 days BMP-4-based medium; B = 21 days BMP-4-based medium; and Bp = 21 days BMP-4-based medium + 48 h IFN-γ and TNF-α. Nonparametric paired Wilcoxon test was used to compare different groups. $*p < 0.05$ and $**p < 0.01$.

Discussion

At least 1 million patients per year need treatment for skeletal disorders, and many of them are treated with bone graft substitutes. The current gold standard for bone regeneration is represented by bone autograft due to its proven osteogenic properties and the lack of immunological rejection. However, this technique has important limitations related to the explant of adequate autologous bone fragments from iliac crest, with associated morbidity for the patients.[8,33] An alternative chance is represented by BTE, which is based on the use of bone substitutes as a scaffold[10] associated to MSC transplantation. If employed alone, both approaches have several limitations related to either the scarce number of residual osteoprogenitor cells[34,35] or the insufficient degree of MSC engraftment and bone formation,[36] respectively. Therefore, the approach combining the two strategies seems to be more promising.[11,12,24] In fact, the scaffold not only provides mechanical stability but also acts as a vehicle actively supporting MSC differentiation into osteoblasts and new bone formation.[37,38]

Since MSCs of different origins are powerful immune regulatory cells, and allogeneic MSCs could be theoretically employed for regenerative medicine in case of lack of autologous cells, it is mandatory to produce preclinical data on MSC immunological properties in presence of the scaffold, before moving into the clinical practice. To this aim, we studied the effect of an HA/TCP scaffold, which has been recently approved as a filler in bone defects by the European Community (EC label), on the immune modulatory effects of MSCs of different origins. We found that the association of HA/TCP with BM-MSCs, ASCs, or CB-MSCs did not affect the MSC immunophenotype and immune modulatory functions. In particular, all the MSC types cultured in presence of the HA/TCP scaffold promoted the survival of resting immune effector cells, while inhibiting the proliferation of activated T and NK cells and, after inflammatory priming, B cells. These features could favor the bone regeneration process *in vivo* by controlling local inflammation in the injury site, without affecting the survival of quiescent immune effector cells.

Some recent reports compared the capabilities of BM-MSCs, ASCs, and CB-MSCs to differentiate into mesodermal tissues, that is, adipocytes, chondrocytes, and osteoblasts.[39–41] Here, we asked whether BM-MSCs, ASCs, and CB-MSCs differ in their expression of RUNX2, one of the pivotal factors driving osteoblast differentiation.[42] We found that BM-MSCs from different donors significantly expressed RUNX2. In contrast, ASCs expressed low levels of RUNX2, while its expression was detectable only in 2/4 CB-MSC samples.

RNA and protein expression analysis showed that BM-MSCs and CB-MSCs possess higher osteogenic differentiation potential as compared with ASCs. Notably, ASCs could be induced only slightly to become mature osteoblasts by DXM-based medium, which instead induced adipogenic differentiation with lipid draft accumulation in 4 out of 5 samples (Fig. 3); this finding could depend on ASC-specific ontogenesis. In addition, some reports showed that ASCs might strongly induce new blood vessel formation and promote bone healing through an indirect mechanism probably related to pro-angiogenic factors.[43] In contrast, BMP-4 addition induced a huge differentiation in BM-MSCs and CB-MSCs. ASCs were also induced by BMP-4 to produce calcium deposition in culture, although less remarkably. The differences among various cell sources could be determined by both tissue origin and culture medium employed for cell expansion. Interestingly, the association of MSCs with HA/TCP, in absence of any differentiation stimulus, induced the transcription of osteoblast-related genes (*OSX* and *OSC*) in BM-MSCs and, to a lesser extent, in ASCs and CB-MSCs, thus confirming the high osteoinductivity of HA/TCP on MSCs, as previously shown in animal models.[44–46] The osteoinductive features of HA/TCP are related to calcium phosphate release, as demonstrated both *in vitro* and *in vivo* by using calcium-deficient HA materials.[47,48]

The adequacy of specific animal models to assess whether allogeneic MSCs may drive new bone formation is still under debate; for instance, mouse MSCs display several important differences from human MSCs, including the immune regulatory mechanisms,[49] and the results cannot be directly transferred into the human setting. The use of humanized animal models, generated by the infusion of allogeneic hematopoietic stem cells in immune deficient mice, may represent a more suitable approach to study the feasibility of MSC therapy in an allogeneic setting.[50]

To produce preclinical *in vitro* data on the feasibility to use allogeneic predifferentiated MSCs in combination with the scaffold, we investigated whether MSC differentiation in the presence of HA/TCP scaffold could affect their immune modulatory properties. ASCs and CB-MSCs retained most of their regulatory features even after BMP-4-mediated differentiation, while BMP-4-differentiated BM-MSCs became less suppressive toward T- and NK-cell proliferation. The latter finding could be related to the higher tendency of BM-MSCs to differentiate into osteoblasts, which do not seem to be immune modulatory.[51,52] Osteoblastic differentiation of BM-MSCs was also evident after a 26 day culture with HA/TCP scaffold, in the absence of DXM or BMP-4, but this partial differentiation was not associated with the loss of inhibitory potential. The balance between bone-depositing osteocyte-like MSCs and immunosuppressive undifferentiated MSCs could be useful, *in vivo*, to promote bone healing and to reduce local inflammation.

We then investigated the molecular mechanisms involved in the inhibition of T-cell proliferation by BMP-4-differentiated MSCs. We found that BMP-4-differentiated BM-MSCs switched on their suppressive machinery by activating both IDO and COX-2, whose role was not significant in human undifferentiated BM-MSCs. PGE2 is produced rapidly as a mediator of inflammation after fracture, and recent data highlighted the role of COX-2 in improving fracture healing. In a multiple tibial fracture mouse model, COX-2 gene therapy increased the number of mesenchymal progenitors within the fracture callus, promoted neoangiogenesis, and improved osteoblastic differentiation of resident MSCs.[53] This phenomenon could also occur in humans, as COX-2 expression by differentiated BM-MSCs could promote the differentiation of neighboring MSCs and trigger the anti-inflammatory effect.

However, fracture healing results from the balance between pro-inflammatory and anti-inflammatory signals. Many groups studied the effect of inflammation on the development

of autoimmune and degenerative diseases associated with impaired healing.[54] Some inflammatory cytokines, such as IFN-γ and TNF-α, may inhibit the differentiation of MSCs into osteoblasts both *in vitro* and *in vivo*[55,56]; on the other hand, the suppression of TNF signaling impairs bone healing *in vivo*.[57] The priming of all MSCs types with IFN-γ and TNF-α before osteoblastic differentiation induced the inhibition of RUNX2 overexpression, unless BMP-4 was used as an osteoblastic inducer. These data support the concept that BMP-4 is a better inducer of osteoblastic differentiation of MSCs as compared with DXM.

Overall, our study gives new clues about MSC biology and some preclinical data supporting the use of allogeneic MSCs in combination with ceramic scaffolds to treat bone defects. The possibility to load the scaffold with bioactive molecules, such as BMPs or VEGF, is currently under investigation to increase both bone regeneration and angiogenesis, preserving a useful degree of anti-inflammatory effects.

Acknowledgments

This work was supported by grants from the seventh Framework Program of the European Commission: CASCADE (FP7-HEALTH-233236) and REBORNE ''Regenerating bone defects using new biomedical approaches'' (FP7-HEALTH-241879) and by grants from the Italian Ministry of University and Scientific Research–PRIN 2009; Ricerca Sanitaria Finalizzata 2008; Cariverona Foundation, Verona, Italy (Bando 2008 e 2012); the European Center for Transplantation Sciences and Immunotherapy (IHU CESTI, ANR-10-IBHU-0005), the Infrastructure Program ECELL-FRANCE (ANR-11-INSB-005), and the CPER 2007–2013 (axe Biothérapie). The authors thank Biomatlante for providing customized HA/TCP discs. The funders had no role in the study design, data collection and analysis, decision to publish, or preparation of this article.

Authors' Contribution

G.B., F.G., and C.M.: conception and design; sample analysis; data collection, analysis, and interpretation; article writing. M.D.T.: sample analysis; data collection and analysis. F.D., L.S., H.S., R.G., P.B., and M.D.: provision of SC samples; data analysis and interpretation. K.T. and M.K.: conception and design; data analysis and interpretation; article writing; final approval.

Disclosure Statement

No competing financial interests exist.

References

1. Okamoto, K., and Takayanagi, H. Regulation of bone by the adaptive immune system in arthritis. Arthritis Res Ther **13,** 219, 2011.
2. Takayanagi, H. Osteoimmunology: shared mechanisms and crosstalk between the immune and bone systems. Nat Rev Immunol **7,** 292, 2007.
3. Schmidt-Bleek, K., Schell, H., Schulz, N., Hoff, P., Perka, C., Buttgereit, F., Volk, H-D., Lienau, J., and Duda, G.N. Inflammatory phase of bone healing initiates the regenerative healing cascade. Cell Tissue Res **347,** 567, 2012.
4. Claes, L., Recknagel, S., and Ignatius, A. Fracture healing under healthy and inflammatory conditions. Nat Rev Rheumatol **8,** 133, 2012.
5. Audigé, L., Griffin, D., Bhandari, M., Kellam, J., and Rüedi, T.P. Path analysis of factors for delayed healing and nonunion in 416 operatively treated tibial shaft fractures. Clin Orthop Relat Res **438,** 221, 2005.
6. Dimitriou, R., Jones, E., McGonagle, D., and Giannoudis P.V. Bone regeneration: current concepts and future directions. BMC Med **9,** 66, 2011.
7. Lin, C.-L., Fang, C.-K., Chiu, F.-Y., Chen, C.-M., and Chen, T.-H. Revision with dynamic compression plate and cancellous bone graft for aseptic nonunion after surgical treatment of humeral shaft fracture. J Trauma **67,** 1393, 2009.
8. Kurz, L.T., Garfin, S.R., and Booth, R.E. Harvesting autogenous iliac bone grafts. A review of complications and techniques. Spine **14,** 1324, 1989.
9. Myeroff, C., and Archdeacon, M. Autogenous bone graft: donor sites and techniques. J Bone Joint Surg Am **93,** 2227, 2011.
10. Bueno, E.M., and Glowacki, J. Cell-free and cell-based approaches for bone regeneration. Nat Rev Rheumatol **5,** 685, 2009.
11. Dupont, K.M., Boerckel, J.D., Stevens, H.Y., Diab, T., Kolambkar, Y.M., Takahata, M., Schwarz, E.M., and Guldberg, R.E. Synthetic scaffold coating with adeno-associated virus encoding BMP2 to promote endogenous bone repair. Cell Tissue Res **347,** 575, 2012.
12. Cordonnier, T., Langonné, A., Sohier, J., Layrolle, P., Rosset, P., Sensébé, L., and Deschaseaux, F. Consistent osteoblastic differentiation of human mesenchymal stem cells with bone morphogenetic protein 4 and low serum. Tissue Eng Part C Methods **17,** 249, 2010.
13. Uccelli, A., Moretta, L., and Pistoia, V. Mesenchymal stem cells in health and disease. Nat Rev Immunol **8,** 726, 2008.
14. Gotherstrom, C., Ringden, O., Tammik, C., Zetterberg, E., Westgren, M., and Le Blanc, K. Immunologic properties of human fetal mesenchymal stem cells. Am J Obstet Gynecol **190,** 239, 2004.
15. Ding, S.J., Shie, M.Y., Hoshiba, T., Kawazoe, N., Chen, G., and Chang, H.C. Osteogenic differentiation and immune response of human bone-marrow-derived mesenchymal stem cells on injectable calcium-silicate-based bone grafts. Tissue Eng Part A **16,** 2343, 2010.
16. Wang, L., Lu, X.F., Lu, Y.R., Liu, J., Gao, K., Zeng, Y.Z., Li, S.F., Li, Y.P., Cheng, J.Q., Tan, W.D., and Wan, L. Immunogenicity and immune modulation of osteogenic differentiated mesenchymal stem cells from Banna minipig inbred line. Transplant Proc **38,** 2267, 2006.
17. Le Blanc, K., Tammik, C., Rosendahl, K., Zetterberg, E., and Ringden, O. HLA expression and immunologic properties of differentiated and undifferentiated mesenchymal stem cells. Exp Hematol **31,** 890, 2003.
18. Le Blanc, K., Frassoni, F., Ball, L., Locatelli, F., Roelofs, H., Lewis, I., Lanino, E., Sundberg, B., Bernardo, M.E., Remberger, M., Dini, G., Egeler, R.M., Bacigalupo, A., Fibbe, W., and Ringdén, O. Mesenchymal stem cells for treatment of steroid-resistant, severe, acute graft-versus-host disease: a phase II study. Lancet **371,** 1579, 2008.
19. Connick, P., Kolappan, M., Crawley, C., Webber, D.J., Patani, R., Michell, A.W., Du, M.-Q., Luan, S.-L.,

Altmann, D.R., Thompson, A.J., Compston, A., Scott, M.A., Miller, D.H., and Chandran, S. Autologous mesenchymal stem cells for the treatment of secondary progressive multiple sclerosis: an open-label phase 2a proof-of-concept study. Lancet Neurol **11,** 150, 2012.

20. Tan, J., Wu, W., Xu, X., Liao, L., Zheng, F., Messinger, S., Sun, X., Chen, J., Yang, S., Cai, J., Gao, X., Pileggi, A., and Ricordi, C. Induction therapy with autologous mesenchymal stem cells in living-related kidney transplants: a randomized controlled trial. JAMA **307,** 1169, 2012.
21. Marini, J.C., and Forlino, A. Replenishing cartilage from endogenous stem cells. N Engl J Med **366,** 2522, 2012.
22. Vacanti, C.A., Bonassar, L.J., Vacanti, M.P., and Shufflebarger, J. Replacement of an avulsed phalanx with tissue-engineered bone. N Engl J Med **344,** 1511, 2001.
23. Xu, J., Wang, W., Ludeman, M., Cheng, K., Hayami, T., Lotz, J.C., and Kapila, S. Chondrogenic differentiation of human mesenchymal stem cells in three-dimensional alginate gels. Tissue Eng Part A **14,** 667, 2008.
24. Cordonnier, T., Layrolle, P., Gaillard, J., Langonné, A., Sensebé, L., Rosset, P., and Sohier, J. 3D environment on human mesenchymal stem cells differentiation for bone tissue engineering. J Mater Sci Mater Med **21,** 981, 2010.
25. Roch, T., Krüger, A., Kratz, K., Ma, N., Jung, F., and Lendlein, A. Immunological evaluation of polystyrene and poly(ether imide) cell culture inserts with different roughness. Clin Hemorheol Microcirc **52,** 375, 2012.
26. Fellah, B.H., Delorme, B., Sohier, J., Magne, D., Hardouin, P., and Layrolle, P. Macrophage and osteoblast responses to biphasic calcium phosphate microparticles. J Biomed Mater Res A **93,** 1588, 2010.
27. Krampera, M., Galipeau, J., Shi, Y., Tarte, T., and Sensebe, L. Immunological characterization of multipotent mesenchymal stromal cells—The International Society for Cellular Therapy (ISCT) working proposal. Cytotherapy **15,** 1054, 2013.
28. Akiyama, K., Chen, C., Wang, D., Xu, X., Qu, C., Yamaza, T., Cai, T., Chen, W., Sun, L., and Shi, S. Mesenchymal-stem-cell-induced immunoregulation involves FAS-ligand-/FAS-mediated T cell apoptosis. Cell Stem Cell **10,** 544, 2012.
29. Benvenuto, F., Ferrari, S., Gerdoni, E., Gualandi, F., Frassoni, F., Pistoia, V., Mancardi, G., and Uccelli, A. Human mesenchymal stem cells promote survival of T cells in a quiescent state. Stem Cells **27,** 1753, 2007.
30. Di Nicola, M., Carlo-Stella, C., Magni, M., Milanesi, M., Longoni, P.D., Matteucci, P., Grisanti, S., and Gianni, A.M. Human bone marrow stromal cells suppress T-lymphocyte proliferation induced by cellular or nonspecific mitogenic stimuli. Blood **99,** 3838, 2002.
31. Menard, C., Pacelli, L., Bassi, G., Dulong, J., Bifari, F., Bezier, I., Zanoncello, J., Ricciardi, M., Latour, M., Bourin, P., Schrezenmeier, H., Sensebé, L., Tarte, K., and Krampera, M. Clinical-grade mesenchymal stromal cells produced under various GMP processes differ in their immunomodulatory properties: standardization of immune quality controls. Stem Cells Dev **22,** 1789, 2013.
32. Fekete, N., Gadelorge, M., Furst, D., Maurer, C., Dausend, J., Fleury-Cappellesso, S., Mailander, V., Lotfi, R., Ignatius, A., Sensebe, L., Bourin, P., Schrezenmeier, H., and Rojewski, M.T. Platelet lysate from whole blood-derived pooled platelet concentrates and apheresis-derived platelet concentrates for the isolation and expansion of human bone marrow mesenchymal stromal cells: production process, content and identification of active components. Cytotherapy **14,** 540, 2012.
33. Khan, Y., Yaszemski, M.J., Mikos, A.G., and Laurencin, C.T. Tissue engineering of bone: material and matrix considerations. J Bone Joint Surg Am **90,** 36, 2008.
34. Petite, H., Viateau, V., Bensaïd, W., Meunier, A., De Pollak, C., Bourguignon, M., Oudina, K., Sedel, L., and Guillemin, G. Tissue-engineered bone regeneration. Nat Biotechnol **18,** 959, 2000.
35. Dupont, K.M., Sharma, K., Stevens, H.Y., Boerckel, J.D., Garcia, A.J., and Guldberg, R.E. Regenerative medicine special feature: human stem cell delivery for treatment of large segmental bone defects. PNAS **107,** 3305, 2010.
36. Gnecchi, M., He, H., Liang, O.D., Melo, L.G., Morello, F., Mu, H., Noiseux, N., Zhang, L., Pratt, R.E., Ingwall, J.S., and Dzau, V.J. Paracrine action accounts for marked protection of ischemic heart by Akt-modified mesenchymal stem cells. Nat Med **11,** 367, 2011.
37. Atkins, G.J., Welldon, K.J., Holding, C.A., Haynes, D.R., Howie, D.W., and Findlay, D.M. The induction of a catabolic phenotype in human primary osteoblasts and osteocytes by polyethylene particles. Biomaterials **30,** 3672, 2009.
38. Lavenus, S., Pilet, P., Guicheux, J., Weiss, P., Louarn, G., and Layrolle, P. Behaviour of mesenchymal stem cells, fibroblasts and osteoblasts on smooth surfaces. Acta Biomater **30,** 1525, 2011.
39. Kern, S., Eichler, H., Stoeve, J., Klüter, H., and Bieback, K. Comparative analysis of mesenchymal stem cells from bone marrow, umbilical cord blood, or adipose tissue. Stem Cells **24,** 1294, 2006.
40. Zhang, Z.-Y., Teoh, S.-H., Hui, J.H.P., Fisk, N.M., Choolani, M., and Chan, J.K.Y. The potential of human fetal mesenchymal stem cells for off-the-shelf bone tissue engineering application. Biomaterials **33,** 2656, 2012.
41. Al-Nbaheen, M., Vishnubalaji, R., Ali, D., Bouslimi, A., Al-Jassir, F., Megges, M., Prigione, A., Adjaye, J., Kassem, M., and Aldahmash, A. Human stromal (mesenchymal) stem cells from bone marrow, adipose tissue and skin exhibit differences in molecular phenotype and differentiation potential. Stem Cell Rev **9,** 32, 2013.
42. Lee, J.-S., Lee, J.-M., and Im, G.-I. Electroporation-mediated transfer of Runx2 and Osterix genes to enhance osteogenesis of adipose stem cells. Biomaterials **32,** 760, 2011.
43. Pinheiro, C.H., de Queiroz, J.C., Guimaraes-Ferreira, L., Vitzel, K.F., Nachbar, R.T., de Sousa, L.G., de Souza-Jr, A.L., Nunes, M.T., and Curi, R. Local injections of adipose-derived mesenchymal stem cells modulate inflammation and increase angiogenesis ameliorating the dystrophic phenotype in dystrophin-deficient skeletal muscle. Stem Cell Rev **8,** 363, 2012.
44. Arinzeh, T.L., Tran, T., Mcalary, J., and Daculsi, G. A comparative study of biphasic calcium phosphate ceramics for human mesenchymal stem-cell-induced bone formation. Biomaterials **26,** 3631, 2005.
45. Habibovic, P., Yuan, H., van der Valk, C.M., Meijer, G., Van Blitterswijk, C.A., and de Groot, K. 3D microenvironment as essential element for osteoinduction by biomaterials. Biomaterials **26,** 3565, 2005.
46. Jégoux, F., Goyenvalle, E., Cognet, R., Malard, O., Moreau, F., Daculsi, G., and Aguado, E. Mandibular segmental defect regenerated with macroporous biphasic calcium phosphate, collagen membrane, and bone marrow graft in dogs. Arch Otolaryngol Head Neck Surg **136,** 971, 2010.

47. Eyckmans, J., Roberts, S.J., Bolander, J., Schrooten, J., Chen, C.S., and Luyten, F.P. Mapping calcium phosphate activated gene networks as a strategy for targeted osteoinduction of human progenitors. Biomaterials **34,** 4612, 2013.
48. Chai, Y.C., Roberts, S.J., Desmet, E., Kerckhofs, G., van Gastel, N., Geris, L., Carmeliet, G., Schrooten, J., and Luyten, F.P. Mechanisms of ectopic bone formation by human osteoprogenitor cells on CaP biomaterial carriers. Biomaterials **33,** 3127, 2012.
49. Ren, G., Su, J., Zhang, L., Zhao, X., Ling, W., L'huillie, A., Zhang, J., Lu, Y., Roberts, A., and Ji, W. Species variation in the mechanisms of mesenchymal stem cell-mediated immunosuppression. Stem Cells **27,** 1954, 2009.
50. Lang, J., Kelly, M., Freed, B.M., McCarter, M.D., Kedl, R.M., Torres, R.M., and Pelanda, R. Studies of lymphocyte reconstitution in a humanized mouse model reveal a requirement of T cells for human B cell maturation. J Immunol **190,** 2090, 2013.
51. Skjødt, H., Møller, T., and Freiesleben, S.F. Human osteoblast-like cells expressing MHC class II determinants stimulate allogeneic and autologous peripheral blood mononuclear cells and function as antigen-presenting cells. Immunology **68,** 416, 1989.
52. Ward, W.G., Gautreaux, M.D., Lippert, D.C., and Boles, C. HLA sensitization and allograft bone graft incorporation. Clin Orthop Relat Res **466,** 1837, 2008.
53. Lau, K.H., Kothari, V., Das, A., Zhang, X.B., and Baylink, D.J. Cellular and molecular mechanisms of accelerated fracture healing by COX2 gene therapy: studies in a mouse model of multiple fractures. Bone **53,** 369, 2013.
54. Martin, P., and Leibovich, S.J. Inflammatory cells during wound repair: the good, the bad and the ugly. Trends Cell Biol **15,** 599, 2005.
55. Huang, H., Zhao, N., Xu, X., Xu, Y., Li, S., Zhang, J., and Yang, P. Dose-specific effects of tumor necrosis factor alpha on osteogenic differentiation of mesenchymal stem cells. Cell Prolif **44,** 420, 2011.
56. Liu, Y., Wang, L., Kikuiri, T., Akiyama, K., Chen, C., Xu, X., Yang, R., Chen, W., Wang, S., and Shi, S. Mesenchymal stem cell-based tissue regeneration is governed by recipient T lymphocytes via IFN-γ and TNF-α. Nat Med **17,** 1594, 2011.
57. Gerstenfeld, L.C., Cho, T.J., Kon, T., Aizawa, T., Tsay, A., Fitch, J., Barnes, G.L., Graves, D.T., and Einhorn, T.A. Impaired fracture healing in the absence of TNF-alpha signaling: the role of TNF-alpha in endochondral cartilage resorption. J Bone Miner Res **18,** 1584, 2003.

Address correspondence to:
Karin Tarte, PhD
INSERM U917
Faculté de Médecine
Université Rennes 1
EFS Bretagne
2 Avenue du Pr Léon Bernard
Rennes 35043
France

E-mail: karin.tarte@univ-rennes1.fr

Mauro Krampera, MD, PhD
Stem Cell Research Laboratory
Section of Hematology
Department of Medicine
University of Verona
Policlinico ''G.B. Rossi''
P.le L.A.Scuro 10
Verona 37134
Italy

E-mail: mauro.krampera@univr.it

Received: May 9, 2014
Accepted: September 15, 2014
Online Publication Date: December 10, 2014